

JPET #138701

Modulation of sarcoplasmic reticulum function by istaroxime (PST2744) in a pressure-overload heart failure model

Marcella Rocchetti, Matteo Alemanni, Gaspare Mostacciuolo, Paolo Barassi, Claudia
Altomare, Riccardo Chisci, Rosella Micheletti, Patrizia Ferrari, Antonio Zaza.

Dipartimento di Biotecnologie e Bioscienze, Università Milano-Bicocca, Milano, Italy
(MR, MA, GM, CA, RC, AZ);

Praxis Sigma-Tau Research Institute, Settimo Milanese, Italy (PB, RM, PF).

JPET #138701

Running title: SR function modulation in heart failure

Corresponding Author:

Antonio Zaza, M.D., F.E.S.C.

Dipartimento di Biotecnologie e Bioscienze, Università degli Studi Milano-Bicocca,
P.zza della Scienza 2, 20126 Milano, Italy

phone: +39 02 64483307; fax: +39 02 64483565

antonio.zaza@unimib.it

Text pages: 34

Tables: 2

Figures: 8

References: 36

Words in the *Abstract*: 244

Words in the *Introduction*: 369

Words in the *Discussion*: 1640

Section: Cardiovascular

List of non-standard abbreviations (in alphabetical order)

AoB	aortic banding
Ca _f	free cytosolic Ca ²⁺ concentration
Ca _{NCX}	Ca ²⁺ moles moving through I _{NCX}
Ca _{rest}	resting Ca ²⁺ at -80 mV
Ca _{SRT}	total sarcoplasmic reticulum Ca ²⁺ content
CICR	Ca ²⁺ -induced Ca ²⁺ release
C _m	membrane electrical capacity
CV	coefficient of variation
dCa/dt _{max}	maximum velocity of Ca ²⁺ rise
HF	hypertrophy/failure
HW/BW	heart weight/body weight ratio
I _{CaL}	L type Ca ²⁺ current
I _{NCX}	Na ⁺ /Ca ²⁺ exchanger current
K _d	dissociation constants (for indo-1 or Ca ²⁺ buffers)
LW/BW	lung weight/body weight ratio
NCX	Na ⁺ /Ca ²⁺ exchanger
PLB	phospholamban
PST2744	(E,Z)-3-((2-Aminoethoxy)imino) androstane-6,17-dione hydrochloride)
R, R _{min} , R _{max}	emission fluorescence ratios (410/490 nm)
RyR	ryanodine receptor
SERCA	sarcoplasmic reticulum Ca-ATPase
SR	sarcoplasmic reticulum
V _{cyt}	volume of cytosol
τ _{decay}	time constant of Ca ²⁺ transient relaxation

JPET #138701

ABSTRACT

Objective: Istaroxime (PST2744) is a novel inotropic agent which enhances SERCA2 activity. We investigated istaroxime effect on Ca^{2+} handling abnormalities in myocardial hypertrophy/failure (HF). **Methods:** guinea-pig myocytes were studied 12 weeks after aortic banding (AoB) and compared to those of sham-operated animals (sham). The gain of calcium-induced Ca^{2+} release (CICR), sarcoplasmic reticulum (SR) Ca^{2+} content, $\text{Na}^+/\text{Ca}^{2+}$ exchanger (NCX) function and the rate of SR reloading after caffeine-induced depletion (SR Ca^{2+} uptake, measured during NCX blockade) were evaluated by measurement of cytosolic Ca^{2+} and membrane currents. **Results:** HF characterization: AoB caused hypertrophy and failure in 100% and 25% of animals respectively. While CICR-gain during constant pacing was preserved, SR Ca^{2+} content and SR Ca^{2+} uptake were strongly depressed. Resting Ca^{2+} and the slope of the $I_{\text{NCX}}/\text{Ca}^{2+}$ relationship were unchanged by AoB. Istaroxime effects: CICR gain, SR Ca^{2+} content and SR Ca^{2+} uptake rate were increased by istaroxime in sham myocytes and, to a significantly larger extent, in AoB myocytes; this led to almost complete recovery of SR Ca^{2+} uptake in AoB myocytes. Istaroxime increased resting Ca^{2+} and the slope of the $I_{\text{NCX}}/\text{Ca}^{2+}$ relationship similarly in sham and AoB myocytes. Istaroxime failed to increase SERCA activity in skeletal muscle microsomes devoid of phospholamban. **Conclusions:** Clear-cut abnormalities in Ca^{2+} handling occurred in this model of hypertrophy with mild decompensation. Istaroxime enhanced SR function more in HF myocytes than in normal ones; almost complete drug-induced recovery suggests a purely functional nature of SR dysfunction in this HF model.

JPET #138701

INTRODUCTION

Positive inotropic interventions remain essential in the management of heart failure; nonetheless their use is strongly limited by proarrhythmic effects and increased oxygen consumption. We have shown that, in normal myocytes, the positive inotropic effect of Na^+/K^+ pump inhibition can be dissociated from proarrhythmia if SERCA2 is stimulated (Rocchetti et al., 2005). The two actions are simultaneously exerted by the compound (E,Z)-3-((2-Aminoethoxy)imino) androstane-6,17-dione hydrochloride (istaroxime, formerly PST2744) whose therapeutic index (inotropy/proarrhythmia) largely exceeds the one of digoxin in single cell and whole animal studies (Micheletti et al., 2002; Rocchetti et al., 2003). The favorable therapeutic profile of istaroxime has been confirmed in animal models of heart failure (Mattera et al., 2007; Sabbah et al., 2007) and in man (Ghali et al., 2007). However, whether this can still be attributed to SERCA2 stimulation is an open question.

Dysfunction of the sarcoplasmic reticulum (SR) is a key feature in myocardial remodelling and is considered as a central mechanism in a wide spectrum of hypertrophy/failure etiologies. Such functional impairment has been variably attributed to downregulation of SERCA2 protein transcription and/or to an increase in the inhibitory (unphosphorylated) form of phospholamban (PLB) (Bers, 2006). Thus, the expression and conformation of the molecular target of istaroxime may be changed in the failing myocardium, with unknown consequences on its effect. At a more general level, the question is how molecular remodelling may affect the response of drugs acting through SERCA2 modulation.

The present study aims to test whether istaroxime is capable of stimulating SR Ca^{2+} uptake also in the presence of cardiac hypertrophy/failure. To this end modulation of Ca^{2+}

JPET #138701

handling by istaroxime was tested in an experimental model of cardiac dysfunction in which chronic pressure overload was induced by aortic constriction in the guinea-pig. The results obtained show that SR impairment can be largely reversed by pharmacological means in this model. This leads to a “functional” interpretation of SERCA2 abnormality, potentially relevant to the therapy of contractile dysfunction. Such an interpretation suggests that istaroxime may act by preventing the interaction between SERCA and PLB. To obtain a preliminary evaluation of this hypothesis, we also tested istaroxime effect on SERCA activity in skeletal muscle microsomes devoid of PLB. This collateral observation is reported in the Supplemental Material.

JPET #138701

METHODS

The investigation conforms to the Guide of the Care and Use of Laboratory Animals published by the US National Institutes of Health (NIH publication No. 85-23, revised 1996) and to the guidelines for animal care endorsed by the hosting institution.

Aortic banding model

Chronic pressure overload was induced in guinea-pigs after banding of the ascending aorta (AoB) under ketamine (100 mg/Kg)-xylazine (5 mg/Kg) intraperitoneally. Sham operated littermates (sham) were used as controls.

Myocyte preparation and recording solutions

Guinea-pigs were killed by cervical dislocation under ketamine-xylazine anesthesia 12 weeks (w) after AoB. Cardiac hypertrophy/heart failure was evaluated through the heart weight/body weight (HW/BW) and lung weight/body weight (LW/BW) ratios. Ventricular myocytes were isolated by using a retrograde coronary perfusion method previously published (Zaza et al., 1998), with minor modifications. Rod shaped, Ca^{2+} tolerant myocytes, were used within 12 h from dissociation.

During measurements myocytes were superfused at 2 ml/min with Tyrode solution containing (mM) 154 NaCl, 4 KCl, 2 CaCl_2 , 1 MgCl_2 , 5 HEPES-NaOH, 5.5 D-glucose, adjusted to pH 7.35. The pipette solution contained (mM) 110 K^+ -aspartate, 23 KCl, 0.2 CaCl_2 (calculated free- $\text{Ca}^{2+} = 10^{-7}$ M), 3 MgCl_2 , 5 HEPES KOH, 0.5 EGTA KOH, 0.4 GTP-Na salt, 5 ATP-Na salt, 5 creatine phosphate Na salt, pH 7.3. Tyrode and pipette solutions were modified for the SR reloading protocol, as detailed in the section on experimental protocols (below). A thermostated manifold, allowing for fast (electronically timed) solution switch, was used for cell superfusion. All measurements were performed at 35 ± 0.5 °C.

JPET #138701

Throughout the present study, istaroxime was tested at the concentration of 4 μM , corresponding to the steep portion of the concentration-response curve for inotropy (Micheletti et al, 2002) and shown to be effective on SR function of normal myocytes of the same species (Rocchetti et al, 2005).

Electrophysiology techniques

Ventricular myocytes were voltage-clamped in the whole-cell configuration (Axopatch 200-A, Axon Instruments). Membrane capacitance (C_m) and series resistance were measured in every cell, but left uncompensated; the average values of series resistance in sham and AoB experiments were $5.1 \pm 0.2 \text{ M}\Omega$ ($N = 48$) and $5.0 \pm 0.2 \text{ M}\Omega$ ($N = 63$) (N.S.) respectively. Current signals were filtered at 2 kHz and digitized at 5 kHz (Axon Digidata 1200). Trace acquisition and analysis was controlled by dedicated software (Axon pClamp 8.0). Guinea-pig ventricular myocytes do not express I_{t_0} (Zicha et al., 2003); thus, peak inward current measured upon depolarizations from a holding potential of -40 mV (I_{Na} fully inactivated) essentially reflects Ca^{2+} influx (through I_{CaL} and I_{NCX}); this was confirmed in preliminary experiments (see Supplemental Figure 1). It is fair to stress that inward current, albeit adequate to calculate CICR-gain (see below), cannot be assumed to reflect I_{CaL} . Indeed, accurate measurement of I_{CaL} requires series resistance compensation, estimation of time-dependent run-down, and intracellular K^+ substitution by Cs^+ , none of which was implemented in the present experiments. In particular, K^+ substitution by Cs^+ was avoided because it affects SR function (Kawai et al., 1998), the main object of this study.

Measurements of intracellular Ca^{2+}

Single myocyte intracellular Ca^{2+} activity was measured fluorimetrically using the membrane permeable dye Indo1-AM (8 μM , Molecular Probes, The Netherlands) as

JPET #138701

previously described. Indo1-AM fluorescent emission was measured at two wavelengths (410 and 490 nm) (Grynkiewicz et al., 1985). The signals at the two wavelengths (F_{410} and F_{490}) were separately lowpass filtered (200 Hz) and digitized at 2 kHz. Cytosolic Ca^{2+} activity was calculated from the F_{410}/F_{490} ratio after lowpass digital filtering (FFT, 100 Hz) and subtraction of the background luminescence. Conversion of F_{410}/F_{490} ratio to free cytosolic Ca^{2+} concentration (Ca_f) was performed as described by Sipido *et al* (Sipido and Callewaert, 1995) after dye calibration in ionomycin permeabilized myocytes (Rocchetti et al, 2005).

Measurement of SERCA activity in SR microsomes

The methods for this set of experiments are reported in the Supplemental Material, where the relevant results are also presented.

Experimental protocols

Protocol 1 (Caffeine pulse protocol): Transmembrane current (holding potential -80 mV) and cytosolic Ca^{2+} were simultaneously recorded (in Tyrode solution) during a 5 s caffeine pulse (10 mM) applied 10 s after a loading train of voltage-steps (-40 to 0 mV, 200 ms, 0.37 Hz).

Protocol 2 (SR reloading protocol): the Na^+/Ca^{2+} -exchanger (NCX) was inhibited by 30 min cells incubation in a Na^+ and Ca^{2+} free solution (replaced by equimolar Li^+ and 1 mM EGTA). SR was initially depleted by a brief caffeine pulse (with 154 mM Na^+ to allow Ca^{2+} extrusion through the NCX) and then progressively reloaded by a train of depolarizing pulses (-40 to 0 mV, 200 ms, 0.25 Hz) in the presence of 1 mM Ca^{2+} (protocol outline at the top of fig 2). The pipette solution was Na^+ -free (Na^+ salts were replaced by K^+ - or Tris- salts).

Estimation of functional parameters

JPET #138701

Total SR Ca^{2+} content (Ca_{SRT} in μmoles per liter of cytosolic volume) was estimated by integrating the $\text{Na}^+/\text{Ca}^{2+}$ exchanger current (I_{NCX}) elicited by the caffeine pulse (protocol 1) and dividing the nmoles of Ca^{2+} by the estimated cell volume ($C_m/6.44$) (Bers, 2002d) (table 1). I_{NCX} was defined as the transient component of caffeine-induced membrane current; thus, the steady state current present during caffeine superfusion (pedestal) was subtracted before integration.

The NCX function was evaluated by plotting I_{NCX} as a function of Ca_f during caffeine pulses (protocol 1, for details see fig 4). The slope of this relation was obtained by linear interpolation of the points in the final third of Ca^{2+} transient relaxation, when bulk cytosolic Ca_f values more closely reflect subsarcolemmal ones (Bers, 2002c) (cells in which the $I_{\text{NCX}}/\text{Ca}_f$ relation was entirely non-linear were not used for this analysis). The steady-state value of Ca_f measured at holding potential just before caffeine application will be referred to as “resting” Ca^{2+} (Ca_{rest}).

The Ca^{2+} -uptake function of SR (SERCA2 uptake flux minus leak flux) was dynamically tested by the SR reloading protocol (protocol 2). The rate of SR reloading was determined from the increment of Ca^{2+} transient amplitude in subsequent voltage steps delivered after caffeine-induced depletion. The time constant of Ca^{2+} transient relaxation (τ_{decay}), reflecting the rate of net SR Ca^{2+} uptake, was measured during each step of the reloading process by monoexponential fit of the Ca^{2+} transient decay. In consideration of the dependency of SERCA2 activity from cytosolic Ca^{2+} (Bers and Berlin, 1995), τ_{decay} was also plotted as a function of peak Ca_f achieved during each step (see Supplemental Figure 2).

The amplification factor in Ca-induced-Ca release (CICR-gain) was calculated according to two methods. In the first one, peak amplitude of Ca^{2+} transient was divided

JPET #138701

by “peak inward current”; in the second one the maximum velocity of Ca^{2+} rise ($d\text{Ca}/dt_{\text{max}}$) was divided by “peak inward current”. Both methods use “peak inward current” in lieu of Ca^{2+} influx, thus yielding a value in arbitrary units (Bers, 2002b). This approach was preferred because an absolute estimate of CICR-gain was beyond the aims of this study and the peak value of inward current may more accurately reflect Ca^{2+} influx under the present experimental conditions. It should be stressed that, because Ca^{2+} release and Ca^{2+} influx are linearly related (Bers, 2002b), their ratio is independent of their absolute value.

Substances

Stock Indo1-AM solution (1 mM in dry DMSO) was diluted in Tyrode solution. Istaroxime was dissolved in water. Istaroxime (PST2744, chemical structure in (Micheletti et al, 2002; Rocchetti et al, 2003) was synthesized at Prassis Sigma-Tau (Settimo Milanese, Italy), Indo-1AM from Molecular Probes (Leiden, The Netherlands), all other chemicals from Sigma (St. Louis, MO, U.S.A.).

Statistical analysis

Sham and AoB conditions are represented by distinct experimental groups; to minimize the effect of inter-subject variability, data were collected from >5 animals in each condition. Sham and AoB animals were studied in alternate sequence. Individual means were compared by paired or unpaired t- test as appropriate; in the SR loading protocol (Figs 2, 6 and Supplemental Figure 2) differences were tested by two-way ANOVA, applied to either absolute values or istaroxime-induced changes. Statistical significance was defined as $p < 0.05$ (N.S. = not significant). The least-square method was used for linear and non-linear fitting and parameter estimation. Data are expressed as mean \pm standard error of independent determinations; the coefficient of variation (CV)

JPET #138701

was calculated as the ratio between standard deviation and mean. Sample size (number of cells) is specified for each experimental condition in the tables and figure legends.

JPET #138701

RESULTS

The evaluations included in this study required the development and characterization of a model of aortic banding in the guinea pig, whose effects have not been previously described. In this section, the observations concerning the functional characterization of the model will be reported first and will be followed by the description of istaroxime effects in sham and AoB animal groups. Results concerning the effect of istaroxime on SERCA activity in microsomes are reported in the Supplemental Material.

Functional characterization of the AoB model

This section of results compares myocardial function of animals 12w after AoB to that of sham of the same gender.

The heart/body weight ratio (HW/BW), lung/body weight ratio (LW/BW) and C_m of sham and AoB animals are compared in table 2. The HW/BW ratio was significantly increased by AoB. There was a tendency to increase of the LW/BW ratio in AoB; while, due to the large scatter, this change did not achieve statistical significance, in 25% of AoB animals the LW/BW ratio was more than 2 fold the average of sham animals. C_m was significantly larger after AoB, to indicate an increase in cell size. Within the study period, mortality was null in both sham and AoB groups.

As shown in figure 1, Ca_{SRT} was decreased by approx 32% after AoB ($p < 0.05$ vs sham) (Fig 1B).

During the SR reloading protocol, the parameters of Ca^{2+} transients (amplitude and τ_{decay}) and the CICR-gain changed over subsequent depolarizing pulses (Fig 2), reflecting a progressive increase in the SR Ca^{2+} content. Thus, the analysis of the time course of these parameters provides information on the SR Ca^{2+} uptake function (Rocchetti et al, 2005). After AoB the time courses of Ca^{2+} -transient amplitude and CICR-gain were

JPET #138701

markedly slowed as compared to sham animals; τ_{decay} was uniformly increased over the whole reloading train (Fig 2B). Differences between sham and AoB myocytes in the time-course of all variables were significant ($p < 0.05$), as tested by two-way ANOVA. The change in τ_{decay} was evident also when compared at similar cytosolic Ca^{2+} concentrations (measured at the beginning of the decay of Ca^{2+} transient, see the Supplemental Figure 2). The changes in Ca^{2+} transient amplitude occurring during the loading protocol and between sham and AoB myocytes (Fig 2A) are accompanied by changes in amplitude and inactivation rate of inward current, as expected from Ca^{2+} -dependent inactivation of I_{CaL} (Lee et al., 1985).

In contrast to the marked depression of SR function detected by the reloading protocol (protocol 2), during steady state stimulation in normal Tyrode (protocol 1) the amplitudes of V-induced Ca^{2+} transients (111.2 ± 11 nM vs. 106.8 ± 9 nM, N.S.), their $d\text{Ca}/dt_{\text{max}}$ (12.7 ± 1.3 nM/ms vs. 13.0 ± 1.0 nM/ms, N.S.) and peak inward current (-4.44 ± 0.32 nA vs. -3.99 ± 0.36 nA, N.S.) were similar between sham and AoB myocytes. Accordingly CICR-gain was unchanged between the two conditions, independently of the method used for its evaluation (Fig 3). The slope of the $I_{\text{NCX}}/\text{Ca}_f$ relation and Ca_{rest} were unchanged by AoB (Fig 4).

Istaroxime effects in sham vs AoB groups

Istaroxime (4 μM) was acutely applied to myocytes from sham and AoB groups and evaluation of functional parameters was performed as above.

In sham myocytes istaroxime effects were similar to those previously reported for normal guinea-pig myocytes (Micheletti et al., 2007; Rocchetti et al, 2005). Istaroxime increased SR Ca^{2+} content by $79.2 \pm 21.1\%$ ($p < 0.05$ vs control; Fig 5). Stimulation of SR Ca^{2+} uptake function by istaroxime was also evident during the SR reloading protocol, in

JPET #138701

which NCX contribution was absent (see methods, protocol 2). Indeed, the rate of change of Ca^{2+} transient amplitude and CICR-gain during the reloading process was increased and τ_{decay} was shortened by the drug (Fig 6). Differences between baseline and istaroxime superfusion in the time-course of all variables were significant ($p < 0.05$), as tested by two-way ANOVA. Consistently with stimulation of SR uptake function, istaroxime increased CICR-gain measured under normal Tyrode superfusion (functioning NCX, Fig 7); istaroxime also increased the slope of the $I_{\text{NCX}}/\text{Ca}_f$ relationship by $93.3 \pm 35\%$ ($p < 0.05$ vs. control, Fig 8) and Ca_{rest} by $41.3 \pm 9.9\%$ ($p < 0.05$ vs. control, Fig 8).

After AoB istaroxime increased Ca_{SRT} by an average of $136.9 \pm 31.9\%$ ($p < 0.05$); although apparently larger, this effect was not significantly different from that observed in sham myocytes ($79.2 \pm 21.1\%$; N.S. vs AoB). Figure 5C shows that failure to achieve significance was due to a wide scatter in istaroxime effect among cells. Rather than being casually variable, istaroxime effect was inversely related to the Ca_{SRT} level measured in control condition, to steeply increase for values below $20 \mu\text{mol/Lcyt}$. Stimulation of SR Ca^{2+} uptake by istaroxime was fully preserved in AoB myocytes, in which baseline SR function was depressed (Fig 6B). Istaroxime effect on the increase in Ca^{2+} transient amplitude during the reloading protocol was actually larger in AoB than in sham myocytes (two-way ANOVA, $p < 0.05$). For the other parameters (τ_{decay} and CICR-gain) istaroxime effect, although highly significant in both groups, was not significantly different between sham and AoB myocytes, probably due to the larger scatter of values. The absolute SR performance achieved under istaroxime in AoB myocytes approached that observed in sham myocytes (Fig 6B), to indicate substantial recovery of AoB-induced dysfunction.

JPET #138701

CICR-gain (measured by protocol 1) was similarly increased by istaroxime in AoB and sham myocytes (Fig 7). The slope of I_{NCX}/Ca_f relationship ($+173 \pm 89\%$), and Ca_{rest} ($+29 \pm 5\%$) were also increased by istaroxime, the effect was again similar between sham and AoB myocytes (Fig 8).

JPET #138701

DISCUSSION

Features of the AoB model

The pressure overload model used in the present study has been previously characterized in vivo at 12 weeks after banding of the ascending aorta, with findings compatible with left ventricular hypertrophy and mild failure (Micheletti et al, 2007); the present ex vivo observations (table 2) are substantially in agreement with in vivo ones. The HW/BW ratio and C_m were consistently increased after AoB, thus reflecting clear-cut myocardial hypertrophy in all cases. Lung congestion was present in a minority of cases. The absence of mortality in the AoB groups rules out the possibility that the hearts used for cell studied may come from a surviving subpopulation, i.e. one with particularly mild abnormalities. Cardiac decompensation observed in the present work is mild as compared to that observed in guinea-pigs studied up to 8 weeks after banding of descending aorta (Ahmmed et al., 2000; Kiss et al., 1995).

The main functional derangement observed in myocytes from AoB animals concerned SR Ca^{2+} uptake function. This was manifested by a marked depression of SR reloading (after caffeine-induced depletion) (Fig 2). Conversely, reduction in SR Ca^{2+} content was relatively milder (-32%; Fig 1) and CICR-gain during steady-state stimulation under normal Tyrode superfusion was unchanged (Fig 3). Considering that SR reloading was measured starting from very a low cell Ca^{2+} content and during NCX blockade, the discrepancy might suggest that the derangement in SR uptake function may be unveiled by low Ca^{2+} content and partially compensated by NCX function. The observation that the reduction of SR Ca^{2+} content was not associated with a decrease in CICR-gain might suggest that the ryanodine receptor (RyR) sensitivity to cytosolic Ca^{2+}

JPET #138701

was increased in AoB myocytes, as commonly observed in the failing heart (Yano et al., 2005).

Abnormality of the SR uptake function, as those detected in this study, can be due to reduced SERCA2 activity, or to increased Ca^{2+} leak through RyR channels. Previous biochemical evaluations showed that maximal ATP-ase activity of SERCA2 is indeed decreased in this model, in spite of normal expression of SERCA2 protein (Micheletti et al, 2007). Reduced SERCA2 activity might result from an increase in the unphosphorylated (monomeric) form of PLB (with no change in the phosphorylated or pentameric fraction), previously described in this model (Micheletti et al, 2007). In this case SERCA2 abnormality would be “functional”, rather than structural, a view also supported by the effect of istaroxime discussed below. This pattern differs from that more often described in hypertrophy, in which a decreased in SERCA2 expression contributes to downregulation of SR Ca^{2+} transport (Bers, 2006).

Ca^{2+} -dependency of I_{NCX} was preserved after AoB (fig 4). This finding is apparently at variance with upregulation of NCX protein expression and enhancement of I_{NCX} reported in human heart failure (Pieske et al., 1999; Studer et al., 1994) and in hypertrophy models in various species, including guinea-pig (Ahmmed et al, 2000). While NCX protein expression was not evaluated in the present work, the functional observations are not necessarily in contrast with previous ones in the same species. Indeed, in the work on guinea-pig by Ahmmed et al. (Ahmmed et al, 2000) I_{NCX} was measured upon repolarization after long depolarizing steps (tail current). An increase in I_{NCX} tail current can be due to either genuine upregulation of NCX function, or simply to an increase in cytosolic Ca^{2+} levels achieved during the depolarizing step (Barceñas-Ruiz et al., 1987). Under the conditions of the study by Ahmmed et al (CICR suppression), the

JPET #138701

latter may be justified in hypertrophied myocytes by depressed SR Ca^{2+} uptake. In the present experiments, NCX function was defined through the relationship between I_{NCX} and cytosolic Ca^{2+} , thus correcting for differences in cytosolic Ca^{2+} level. Nevertheless, in species other than guinea-pigs the same analysis detected an increase of NCX function in hypertrophy (Diaz et al., 2004); thus, it is difficult to rule out that differences in NCX function between this and previous studies may be real and possibly related to the severity of hemodynamic overload.

Istaroxime effects in sham and AoB myocytes

In myocytes from sham operated animals istaroxime improved Ca^{2+} handling, as previously reported in normal hearts of the same species (Rocchetti et al, 2005). Under ionic conditions in which all Ca^{2+} handling mechanisms were operative (normal Tyrode), istaroxime increased total SR Ca^{2+} content (Fig 5), which implies a shift of the balance between Ca^{2+} uptake by SR and Ca^{2+} extrusion from the cell. In turn, SR Ca^{2+} uptake rate reflects the balance between active Ca^{2+} transport (by SERCA2) and passive Ca^{2+} leak through RyR channels, both fluxes being enhanced by high cytosolic Ca^{2+} (Meissner and Henderson, 1987; Shannon et al., 2000). As shown by previous studies in intact myocytes and isolated SR vesicles, istaroxime actions include inhibition of the Na^+/K^+ pump and stimulation of SERCA2 ATP-ase activity (Rocchetti et al, 2003; Rocchetti et al, 2005) (see also the Supplemental Material). While both these actions may concur to increase SR Ca^{2+} content, the former depends on the change in NCX electrochemical equilibrium, secondary to elevation of cytosolic Na^+ . When tested under conditions of complete inhibition of NCX function (Na^+ -free conditions), istaroxime was still able to stimulate SR Ca^{2+} uptake, as reflected by an increase in the rate at which SR reloads after depletion and by an acceleration of Ca^{2+} decay after voltage-induced transients (Fig 6). These

JPET #138701

observations suggest that istaroxime-induced increase in SR Ca^{2+} content may also occur through SERCA2 stimulation, i.e. independently of Na^+/K^+ pump inhibition. Istaroxime also increased the efficacy by which Ca^{2+} influx triggers SR Ca^{2+} release (CICR-gain) (Fig 7), probably an effect secondary to the increase in luminal SR Ca^{2+} (Rocchetti et al, 2005; Xu and Meissner, 1998). Istaroxime increased both the x-axis intercept (Ca_f at $I_{\text{NCX}}=0$) and the slope of the $I_{\text{NCX}}/\text{Ca}_f$ relationship (Fig 8). The intercept change may result from an increase in cytosolic Na^+ and was expected from istaroxime effect on the Na^+/K^+ pump (Rocchetti et al, 2003). According to previous evidence, istaroxime does not directly stimulate NCX (Rocchetti et al, 2003); thus, the increase in the slope of the $I_{\text{NCX}}/\text{Ca}_f$ relationship is more likely due to allosteric modulation of the exchanger by elevated Ca_f (Weber et al., 2001). The net effect of these two changes is a reduction in the rate of Ca^{2+} extrusion through NCX at resting membrane potential (-80 mV).

The rather severe SR dysfunction observed after AoB was almost completely reversed by istaroxime (Figs 5 and 6). This implies that the dysfunction was exclusively “functional” and is consistent with the lack of SERCA2 protein downregulation in this model (Micheletti et al, 2007).

Istaroxime effect in skeletal vs cardiac SR microsomes

The ability of istaroxime to recover the SR abnormality in AoB myocytes suggests that this agent may interfere with SERCA modulation by PLB. This is also consistent with the finding that istaroxime stimulates SERCA2 in cardiac microsomes from healthy guinea pig by increasing its affinity for cytosolic Ca^{2+} (Rocchetti et al, 2005) (Micheletti et al, 2007) (see also Supplemental Material and Supplemental Figure 4), which is limited by the interaction with PLB (Waggoner et al., 2007).

JPET #138701

The observation, reported in the Supplemental Material that istaroxime was unable to increase SERCA activity in skeletal muscle microsomes, which are naturally devoid of PLB, provides a preliminary support to this view (Supplemental Figures 3-4). Albeit suggestive, this observation may not be conclusive and further experiments with a different strategy may be required to confirm the hypothesis.

Practical implications

The majority of evidence available to date, mostly from studies in transgenic animals, identifies recovery of SR Ca^{2+} uptake function as a promising therapeutic strategy in heart failure (Haghighi et al., 2004;Schmidt et al., 2001); however, adverse effects have also been reported (Chen et al., 2004;Vangheluwe et al., 2006). The net outcome of this approach probably depends on the extent of SR uptake enhancement, which may be difficult to adjust if gene-therapy is used. Under this aspect, availability of pharmacological tools for modulation of SR function would be highly desirable; however, it is unclear whether deranged SR function can be recovered by pharmacological means. Previous studies in animal models (Mattera et al, 2007;Micheletti et al, 2007;Sabbah et al, 2007) and man (Ghali et al, 2007) showed that the positive inotropic effect of istaroxime is retained in the failing myocardium, but it was unknown whether stimulation of SR Ca^{2+} uptake could still contribute to it. The present results not only prove that this is indeed the case, but show that almost complete recovery of failing SR uptake function might be achieved by pharmacological means. Beside contractility, SR function may also affect myocardial electrical stability. Istaroxime is also a Na^+/K^+ pump inhibitor, but it is definitely less proarrhythmic than digoxin in animal studies (Micheletti et al, 2002;Rocchetti et al, 2003) and preliminary clinical evidence corroborates this finding (Ferrari et al., 2007;Ghali et al, 2007). The

JPET #138701

electrophysiological actions of the two substances have been thoroughly compared (Rocchetti et al, 2003) and the only mechanism found to account for the different arrhythmogenicity is stimulation of SR Ca^{2+} uptake (Rocchetti et al, 2005). This suggests that contractile recovery is not the only goal which may be achieved by modulation of SR function. The mechanism by which SR stimulation by istaroxime improves electrical stability is currently under evaluation.

Study limitations

In the specific hypertrophy model used by this study, decreased SERCA2 activity occurs in the presence of normal SERCA2 protein expression (Micheletti et al, 2007) and this may represent a prerequisite for functional recovery by pharmacological means. This might prevent full extrapolation of the present findings to conditions in which SERCA2 expression is reduced. Nevertheless, a decrease in the ratio between SERCA2 and (unphosphorylated) PLB is general feature of the failing myocardium (Haghighi et al, 2004), thus suggesting that functional downregulation may have a general role in SR dysfunction. Thus, significant, even if incomplete, recovery might theoretically be achieved by pharmacological means in most cases.

JPET #138701

ACKNOWLEDGEMENTS

We are grateful to Prof. Giuseppe Bianchi for providing constructive discussion throughout the execution of the study, Dr. Bruno Gavillet for reviewing the manuscript, Dr Fiorentina Palazzo and Dr Barbara Moro for guinea-pig aortic banding, Dr Mara Ferrandi for western blot experiments (Supplemental Figure 3).

JPET #138701

REFERENCES

Ahmed GU, Dong PH, Song G, Ball NA, Xu Y, Walsh RA, and Chiamvimonvat N (2000) Changes in Ca²⁺ cycling proteins underlie cardiac action potential prolongation in a pressure-overloaded guinea pig model with cardiac hypertrophy and failure. *Circ.Res.* 86:558-570.

Barceñas-Ruiz L, Beuckelmann DJ, and Wier WG (1987) Sodium-calcium exchange in heart: membrane currents and changes in [Ca²⁺]_i. *Science* 238:1720-1722.

Bers DM (2002a) Ca sources & sinks, in *Excitation-contraction coupling and cardiac contractile force* (Bers DM ed) pp 39-62, Kluwer Academic Publishers, Boston.

Bers DM (2002b) Excitation-contraction coupling, in *Excitation-contraction coupling and cardiac contractile force* (Bers DM ed) pp 203-244, Kluwer Academic Publishers, Boston.

Bers DM (2002c) Sarcolemmal Na/Ca exchange and Ca-pump, in *Excitation-contraction coupling and cardiac contractile force* (Bers DM ed) pp 133-160, Kluwer Academic Publishers, Boston.

Bers DM (2002d) Ultrastructure, in *Excitation-contraction coupling and cardiac contractile force* (Bers DM ed) pp 1-18, Kluwer Academic Publishers, Boston.

Bers DM (2006) Altered cardiac myocyte Ca regulation in heart failure. *Physiology.(Bethesda.)* 21:380-387.

Bers DM and Berlin JR (1995) Kinetics of [Ca]_i decline in cardiac myocytes depend on peak [Ca]_i. *Am J Physiol* 268:C271-C277.

JPET #138701

Chen Y, Escoubet B, Prunier F, Amour J, Simonides WS, Vivien B, Lenoir C, Heimburger M, Choqueux C, Gellen B, Riou B, Michel JB, Franz WM, and Mercadier JJ (2004) Constitutive cardiac overexpression of sarcoplasmic/endoplasmic reticulum Ca²⁺-ATPase delays myocardial failure after myocardial infarction in rats at a cost of increased acute arrhythmias. *Circulation* 109:1898-1903.

Diaz ME, Graham HK, and Trafford AW (2004) Enhanced sarcolemmal Ca²⁺ efflux reduces sarcoplasmic reticulum Ca²⁺ content and systolic Ca²⁺ in cardiac hypertrophy. *Cardiovasc.Res.* 62:538-547.

Ferrari P, Micheletti R, Valentini G, and Bianchi G (2007) Targeting SERCA2a as an innovative approach to the therapy of congestive heart failure. *Med.Hypotheses* 68:1120-1125.

Ghali JK, Smith WB, Torre-Amione G, Haynos W, Rayburn BK, Amato A, Zhang D, Cowart D, Valentini G, Carminati P, and Gheorghiade M (2007) A phase 1-2 dose-escalating study evaluating the safety and tolerability of istaroxime and specific effects on electrocardiographic and hemodynamic parameters in patients with chronic heart failure with reduced systolic function. *Am.J.Cardiol.* 99:47A-56A.

Grynkiewicz G, Poenie M, and Tsien RY (1985) A new generation of Ca²⁺ indicators with greatly improved fluorescence properties. *J Biol Chem* 260:3440-3450.

Haghighi K, Gregory KN, and Kranias EG (2004) Sarcoplasmic reticulum Ca-ATPase-phospholamban interactions and dilated cardiomyopathy. *Biochem.Biophys.Res.Commun.* 322:1214-1222.

JPET #138701

Kawai M, Hussain M, and Orchard CH (1998) Cs⁺ inhibits spontaneous Ca²⁺ release from sarcoplasmic reticulum of skinned cardiac myocytes. *Am J Physiol* 275:H422-H430.

Kiss E, Ball NA, Kranias EG, and Walsh RA (1995) Differential changes in cardiac phospholamban and sarcoplasmic reticular Ca(2+)-ATPase protein levels. Effects on Ca²⁺ transport and mechanics in compensated pressure-overload hypertrophy and congestive heart failure. *Circ.Res.* 77:759-764.

Lee KS, Marban E, and Tsien RW (1985) Inactivation of calcium channels in mammalian heart cells: joint dependence on membrane potential and intracellular calcium. *J Physiol* 364:395-411.

Mattera GG, Lo GP, Loi FM, Vanoli E, Gagnol JP, Borsini F, and Carminati P (2007) Istaroxime: a new luso-inotropic agent for heart failure. *Am.J.Cardiol.* 99:33A-40A.

Meissner G and Henderson JS (1987) Rapid calcium release from cardiac sarcoplasmic reticulum vesicles is dependent on Ca²⁺ and is modulated by Mg²⁺, adenine nucleotide, and calmodulin. *J.Biol.Chem.* 262:3065-3073.

Micheletti R, Mattera GG, Rocchetti M, Schiavone A, Loi MF, Zaza A, Gagnol RJ, De Munari S, Melloni P, Carminati P, Bianchi G, and Ferrari P (2002) Pharmacological profile of the novel inotropic agent (E,Z)-3-((2- aminoethoxy)imino)androstane-6,17-dione hydrochloride (PST2744). *J Pharmacol Exp Ther* 303:592-600.

Micheletti R, Palazzo F, Barassi P, Giacalone G, Ferrandi M, Schiavone A, Moro B, Parodi O, Ferrari P, and Bianchi G (2007) Istaroxime, a stimulator of sarcoplasmic

JPET #138701

reticulum calcium adenosine triphosphatase isoform 2a activity, as a novel therapeutic approach to heart failure. *Am.J.Cardiol.* 99:24A-32A.

Pieske B, Maier LS, Bers DM, and Hasenfuss G (1999) Ca²⁺ handling and sarcoplasmic reticulum Ca²⁺ content in isolated failing and nonfailing human myocardium. *Circ.Res.* 85:38-46.

Rocchetti M, Besana A, Mostacciuolo G, Ferrari P, Micheletti R, and Zaza A (2003) Diverse toxicity associated with cardiac Na⁺/K⁺ pump inhibition: evaluation of electrophysiological mechanisms. *J Pharmacol Exp Ther* 305:765-771.

Rocchetti M, Besana A, Mostacciuolo G, Micheletti R, Ferrari P, Sarkozi S, Szegedi C, Jona I, and Zaza A (2005) Modulation of Sarcoplasmic Reticulum Function by Na⁺/K⁺ Pump Inhibitors with Different Toxicity: Digoxin and PST2744 [(E,Z)-3-((2-Aminoethoxy)imino)androstane-6,17-dione Hydrochloride]. *J.Pharmacol.Exp.Ther.* 313:207-215.

Sabbah HN, Imai M, Cowart D, Amato A, Carminati P, and Gheorghide M (2007) Hemodynamic properties of a new-generation positive lusio-inotropic agent for the acute treatment of advanced heart failure. *Am.J.Cardiol.* 99:41A-46A.

Schmidt AG, Edes I, and Kranias EG (2001) Phospholamban: a promising therapeutic target in heart failure? *Cardiovasc.Drugs Ther.* 15:387-396.

Shannon TR, Ginsburg KS, and Bers DM (2000) Reverse mode of the sarcoplasmic reticulum calcium pump and load- dependent cytosolic calcium decline in voltage-clamped cardiac ventricular myocytes. *Biophys.J.* 78:322-333.

JPET #138701

Sipido KR and Callewaert G (1995) How to measure intracellular $[Ca^{2+}]$ in single cardiac cells with fura-2 or indo-1. *Cardiovasc.Res.* 29:717-726.

Studer R, Reinecke H, Bilger J, Eschenhagen T, Bohm M, Hasenfuss G, Just H, Holtz J, and Drexler H (1994) Gene expression of the cardiac Na^{+} and Ca^{2+} exchanger in end stage human heart failure. *Circ.Res.* 75:443-453.

Vangheluwe P, Tjwa M, Van Den BA, Louch WE, Beullens M, Dode L, Carmeliet P, Kranias E, Herijgers P, Sipido KR, Raeymaekers L, and Wuytack F (2006) A SERCA2 pump with an increased Ca^{2+} affinity can lead to severe cardiac hypertrophy, stress intolerance and reduced life span. *J.Mol.Cell Cardiol.* 41:308-317.

Waggoner JR, Huffman J, Froehlich JP, and Mahaney JE (2007) Phospholamban inhibits Ca -ATPase conformational changes involving the E2 intermediate. *Biochemistry* 46:1999-2009.

Weber CR, Ginsburg KS, Philipson KD, Shannon TR, and Bers DM (2001) Allosteric regulation of Na/Ca exchange current by cytosolic Ca in intact cardiac myocytes. *J.Gen.Physiol* 117:119-131.

Xu L and Meissner G (1998) Regulation of cardiac muscle Ca^{2+} release channel by sarcoplasmic reticulum lumenal Ca^{2+} . *Biophys.J.* 75:2302-2312.

Yano M, Ikeda Y, and Matsuzaki M (2005) Altered intracellular Ca^{2+} handling in heart failure. *J.Clin.Invest* 115:556-564.

JPET #138701

Zaza A, Rocchetti M, Brioschi A, Cantadori A, and Ferroni A (1998) Dynamic Ca^{2+} -induced inward rectification of K^+ current during the ventricular action potential. *Circ.Res.* 82:947-956.

Zicha S, Moss I, Allen B, Varro A, Papp J, Dumaine R, Antzelevitch C, and Nattel S (2003) Molecular basis of species-specific expression of repolarizing K^+ currents in the heart. *Am.J.Physiol Heart Circ.Physiol* 285:H1641-H1649.

JPET #138701

FOOTNOTES

Financial support:

This work was funded by Istituto di Ricerche Prassis Sigma-Tau and from academic funding to A. Zaza. The content of this manuscript was partially presented in abstract form.

Reprint requests to:

Antonio Zaza, M.D., F.E.S.C.

Dipartimento di Biotecnologie e Bioscienze, Università degli Studi Milano-Bicocca,

P.zza della Scienza 2, 20126 Milano, Italy

JPET #138701

LEGENDS FOR FIGURES

FIGURE 1: AoB effect on total SR Ca^{2+} content (Ca_{SRT}). A) Representative examples of caffeine-induced Na^+/Ca^{2+} exchanger current (I_{NCX}) (holding potential -80 mV) and the corresponding cumulative I_{NCX} integrals in a sham (left panels) and AoB (right panels) myocyte. B) Average results of Ca_{SRT} , (see table 1 for method), in sham (N = 30) and AoB (N = 28) myocytes; * = $p < 0.05$ vs sham.

FIGURE 2: AoB effect on SR function (with blocked NCX). A) Example of free cytosolic Ca^{2+} concentration (Ca_f) and membrane current (I_m) recorded during SR reloading after caffeine-induced SR depletion in sham (●) and AoB (▲) myocytes; recordings were performed in the absence of NCX function (Na^+ free Tyrode and pipette solutions). B) Average values of Ca^{2+} transient parameters measured during each pulse (#1 to #6) of the stimulation train in sham (●, N = 23) and AoB (▲, N = 22) myocytes. CICR-gain (measured as the ratio between the Ca^{2+} transient amplitude and the peak inward current) was expressed in arbitrary units (a.u.) (see Methods). Inset: outline of the experimental protocol. Significance of AoB-induced changes was detected by two-way ANOVA ($p < 0.05$ for all variables).

FIGURE 3: AoB effect on CICR-gain. A) Free cytosolic Ca^{2+} concentration (Ca_f) and membrane current (I_m) simultaneously recorded during voltage steps (from -40 to 0 mV for 200 ms) in a sham (left panels) and AoB (right panels) myocyte. B) Average values of CICR-gain (calculated according to two methods and expressed in arbitrary units, a.u., see Methods) in sham (N = 33) and AoB (N = 27) myocytes; dCa/dt_{max} was calculated during the rising phase of the Ca^{2+} transient (boxes in panel A).

FIGURE 4: AoB effect on NCX function. A), B) Free cytosolic Ca^{2+} concentration (Ca_f) and the Na^+/Ca^{2+} exchanger current (I_{NCX}) simultaneously recorded during caffeine

JPET #138701

superfusion (holding potential -80 mV) in a sham (left panels) and AoB (right panels) myocyte; $I_{\text{NCX}}/\text{Ca}_f$ relationship and the linear interpolation of the points in the final third of Ca^{2+} transient relaxation (continuous line) are shown in the insets. C) Average results of the slope of the $I_{\text{NCX}}/\text{Ca}_f$ relationship and resting Ca^{2+} measured at -80 mV (Ca_{rest}) in sham (N = 24) and AoB (N = 24) myocytes.

FIGURE 5: Istaroxime effects in sham vs AoB groups: total SR Ca^{2+} content (Ca_{SRT}).

A), B) Representative example of istaroxime (IST 4 μM , \circ) effect on caffeine-induced $\text{Na}^+/\text{Ca}^{2+}$ exchanger current (I_{NCX}) (holding potential -80 mV) and the corresponding cumulative I_{NCX} integrals in a sham and AoB myocyte. C) IST effect ($\Delta\%$ increase of Ca_{SRT}) as a function of Ca_{SRT} level measured in control (cont, \bullet) in all experimental conditions (data from sham (\blacktriangle , N = 15) and AoB (\triangle , N = 18) groups were pooled together); continuous line represents the best exponential fit of the experimental data.

FIGURE 6: Istaroxime effects in sham vs AoB groups: SR function with blocked NCX.

A) Example of free cytosolic Ca^{2+} concentration (Ca_f) and membrane current (I_m) recorded in a AoB myocyte during SR reloading after caffeine-induced SR depletion in control (cont, \bullet) and after istaroxime superfusion (IST 4 μM , \circ); recordings were performed in the absence of NCX function (Na^+ free Tyrode and pipette solutions); the protocol is outlined in figure 2. B) Average values of Ca^{2+} transient parameters measured during each of the first 6 pulses (#1 to #6) of the stimulation train in cont (\bullet) and after IST superfusion (\circ), in sham (N = 11) and AoB (N = 8) myocytes. The decay time constant (τ_{decay}) was estimated by a monoexponential fit of the Ca^{2+} transient decay; CICR-gain (measured as the ratio between the Ca^{2+} transient amplitude and the peak inward current) was expressed in arbitrary units (a.u). Significance of istaroxime effects

JPET #138701

was tested by two-way ANOVA on all variables for both sham and AoB groups (see text).

FIGURE 7: Istaroxime effects in sham vs AoB groups: CICR-gain. A) Free cytosolic Ca^{2+} concentration (Ca_f) and membrane current (I_m) simultaneously recorded during voltage steps (from -40 to 0 mV for 200 ms) in a sham myocyte, in control (cont) and after istaroxime superfusion (IST 4 μM). B). Average values of CICR-gain (calculated according to two methods and expressed in arbitrary units, a.u., see Methods) in control and after IST superfusion in sham (N = 13) and AoB (N = 17) myocytes; $d\text{Ca}/dt_{\text{max}}$ was calculated during the rising phase of the Ca^{2+} transient (boxes in panel A). * = $p < 0.05$ vs cont.

FIGURE 8: Istaroxime effects in sham vs AoB groups: NCX function. A) Free cytosolic Ca^{2+} concentration (Ca_f) and the $\text{Na}^+/\text{Ca}^{2+}$ exchanger current (I_{NCX}) simultaneously recorded in a sham myocyte during caffeine superfusion (holding potential -80 mV) in control (cont, ●) and after istaroxime superfusion (IST 4 μM , ○); Ca_f and I_{NCX} traces recorded in cont and IST were time aligned for clarity; I_{NCX} traces were also offset to 0 level at the end of caffeine pulse. B) $I_{\text{NCX}}/\text{Ca}_f$ relationships and the linear interpolation of the points in the final third of Ca^{2+} transient relaxation (continuous lines). C), D) Average results of the slope of the $I_{\text{NCX}}/\text{Ca}_f$ relationship and resting Ca^{2+} measured at -80 mV (Ca_{rest}) in cont and after IST superfusion in sham (N = 8) and AoB (N = 11) myocytes; * = $p < 0.05$ vs cont.

JPET #138701

Table 1: Glossary of symbols and method of calculation

Symbol	Meaning	Formula	Parameters	References
Ca _f	Free cyt. Ca ²⁺ (molar concentration)	$K_d * \beta * \frac{R - R_{\min}}{R_{\max} - R}$	K _d = 250 nM; R _{min} =0.24; R _{max} = 0.86; β=2.54	(Grynkiewi cz et al, 1985); from dye calibration
Ca _{NCX}	Ca ²⁺ through I _{NCX} (moles)	$1/zF * \int dI_m * dt$	z=1; F=Faraday constant	(Bers, 2002a)
Ca _{SRT}	SR Ca ²⁺ content (moles/Lcyt.)	$\frac{Ca_{NCX}}{V_{cyt}}$	Ca _{NCX} from caffeine pulse; V _{cyt} = C _m /6.44	(Bers, 2002a)

C_m = membrane capacitance; cyt. = cytosol; I_m = membrane current; K_d = dissociation constants; R_{min}, R_{max} and β= indo-1 calibration parameters (Grynkiewicz et al, 1985); V_{cyt} = volume of cytosol.

JPET #138701

Table 2: AoB model parameters

	HW/BW (g/Kg)		LW/BW (g/Kg)		C _m (pF)	
		CV		CV		CV
sham (n=8)	4.37 ± 0.24	0.16	5.24 ± 0.32	0.17	216 ± 14 (N=48)	0.46
AoB (n=12)	6.56 ± 0.50 *	0.25	5.95 ± 0.82	0.50	303 ± 14 (N=63) *	0.38

HW/BW = heart weight/body weight ratio; LW/BW = lung weight/body weight ratio; C_m = cell membrane capacitance; CV = coefficient of variation; * = p<0.05 vs sham animals; n = # of animals; N = # of cells.

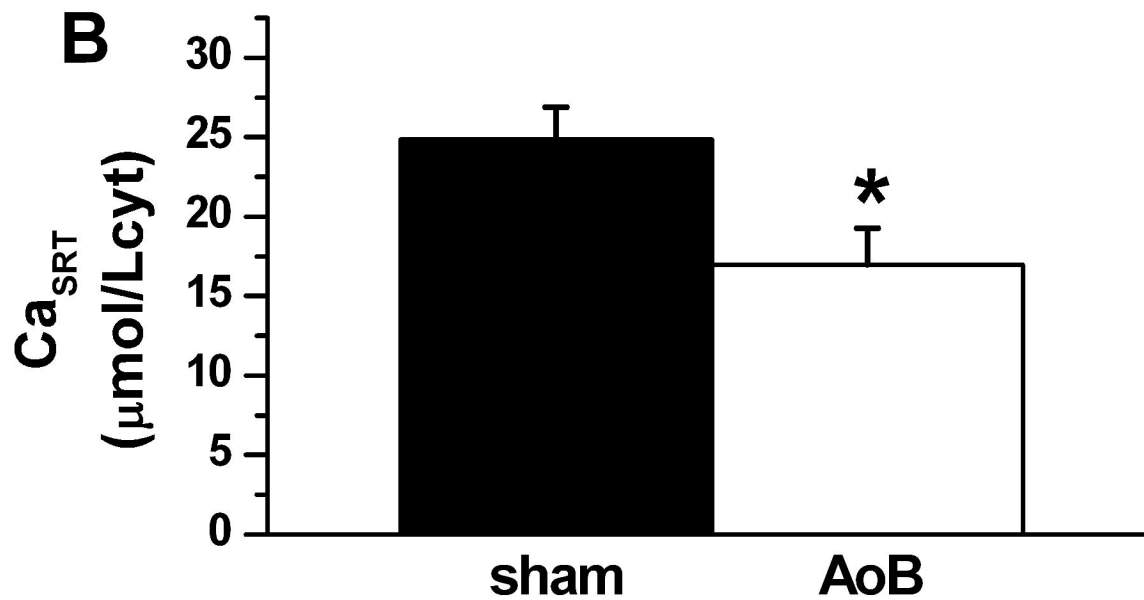
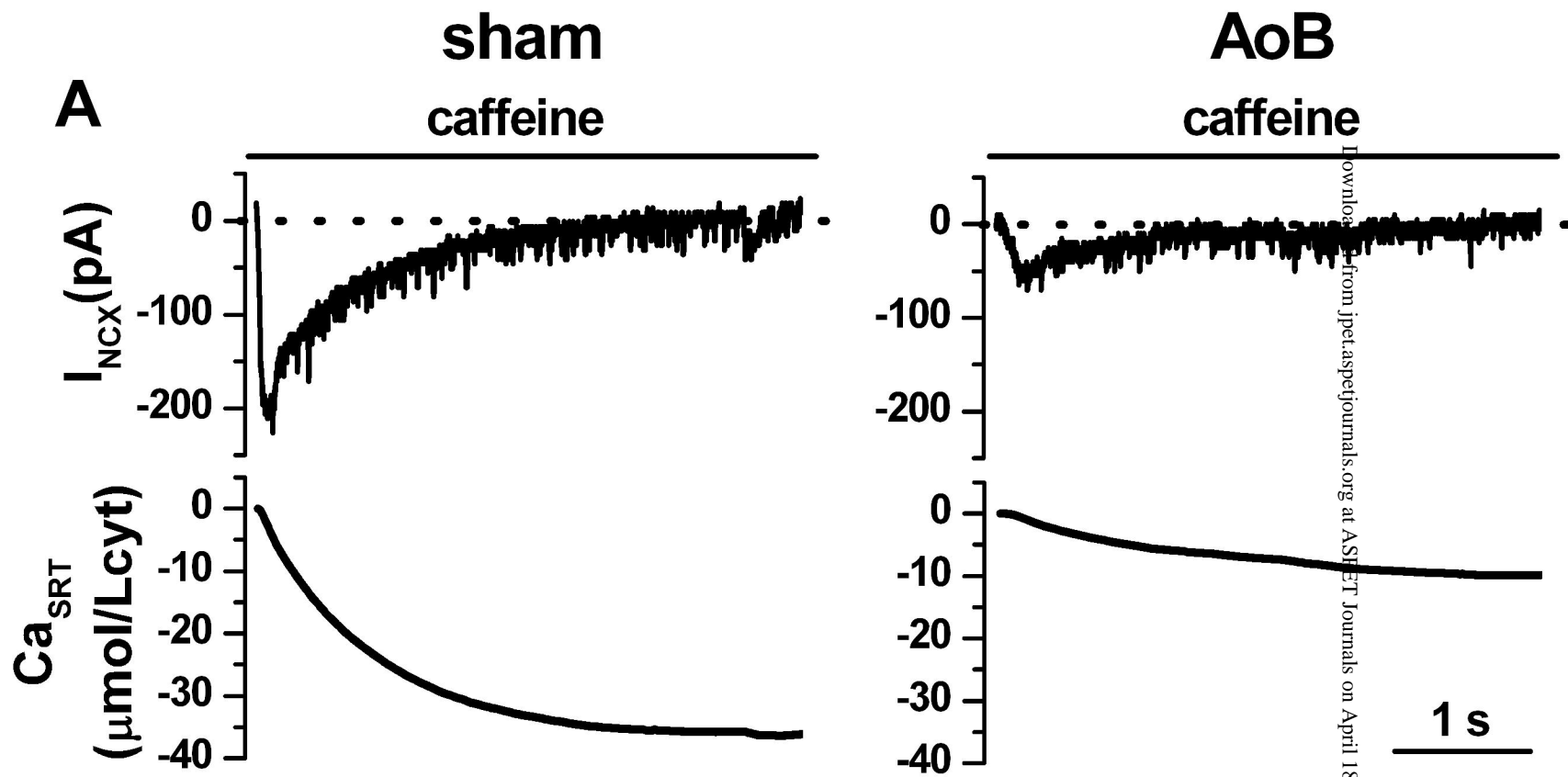


Fig 1

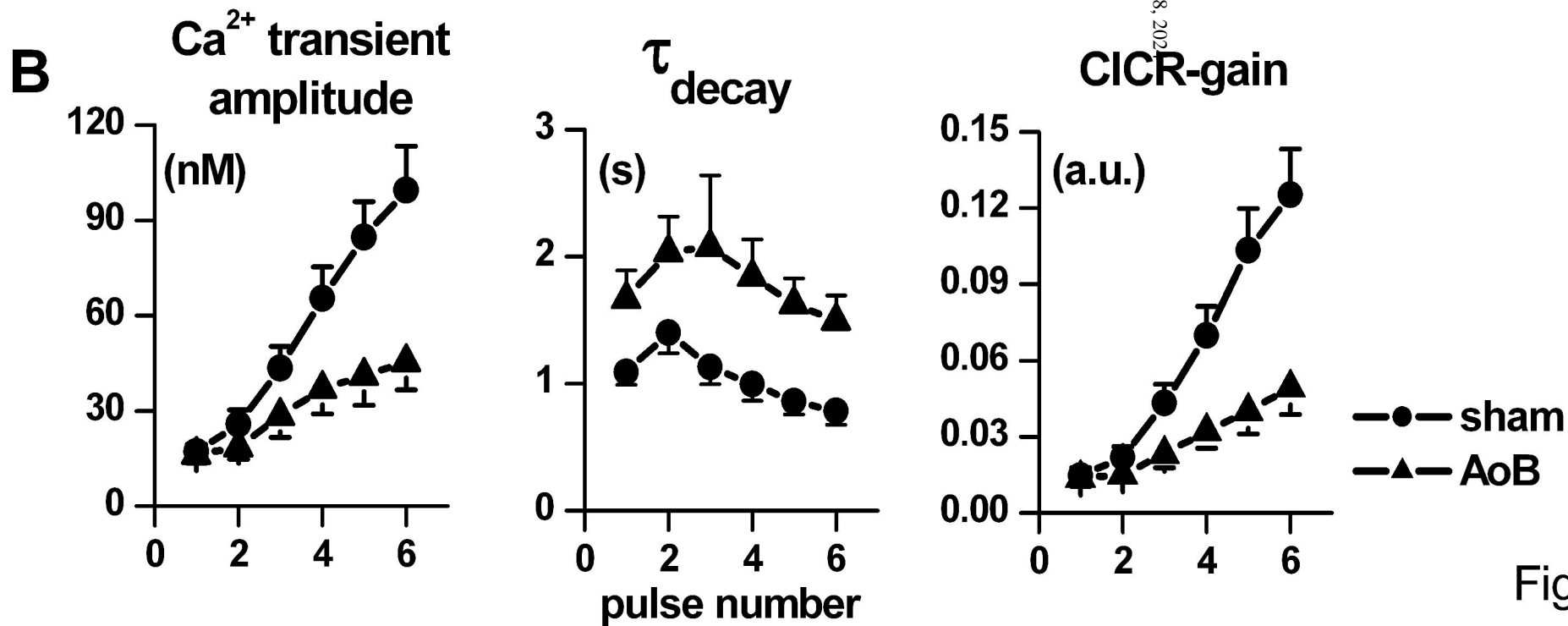
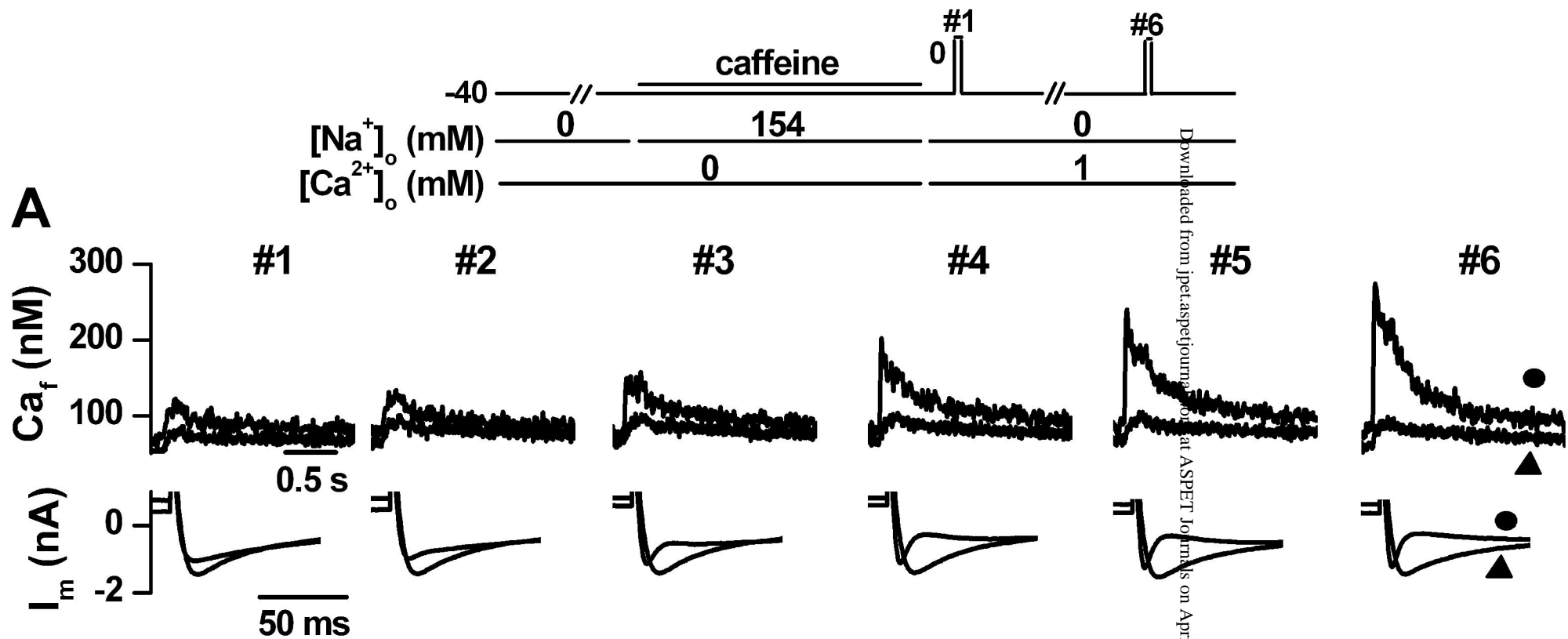


Fig 2

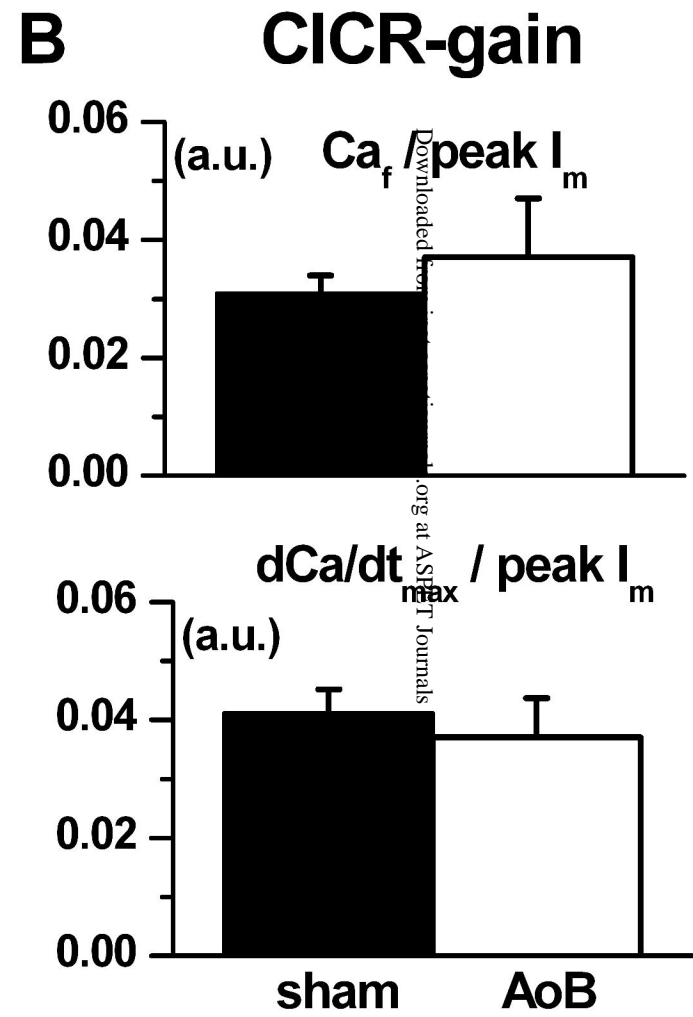
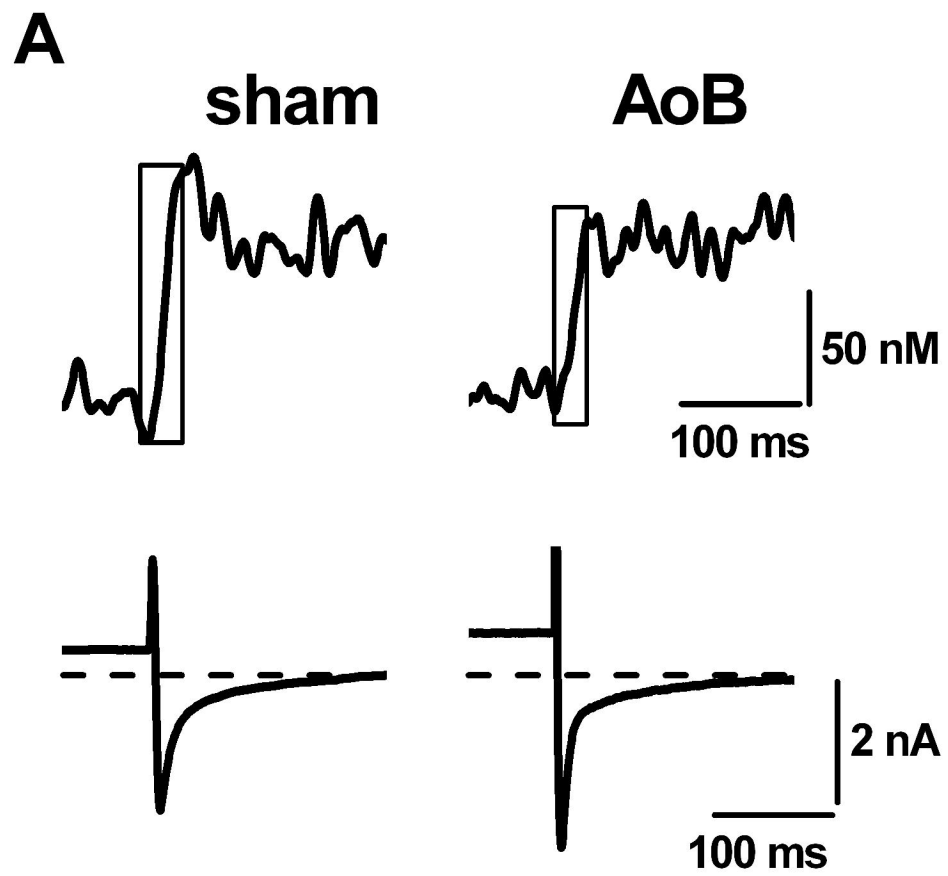


Fig 3

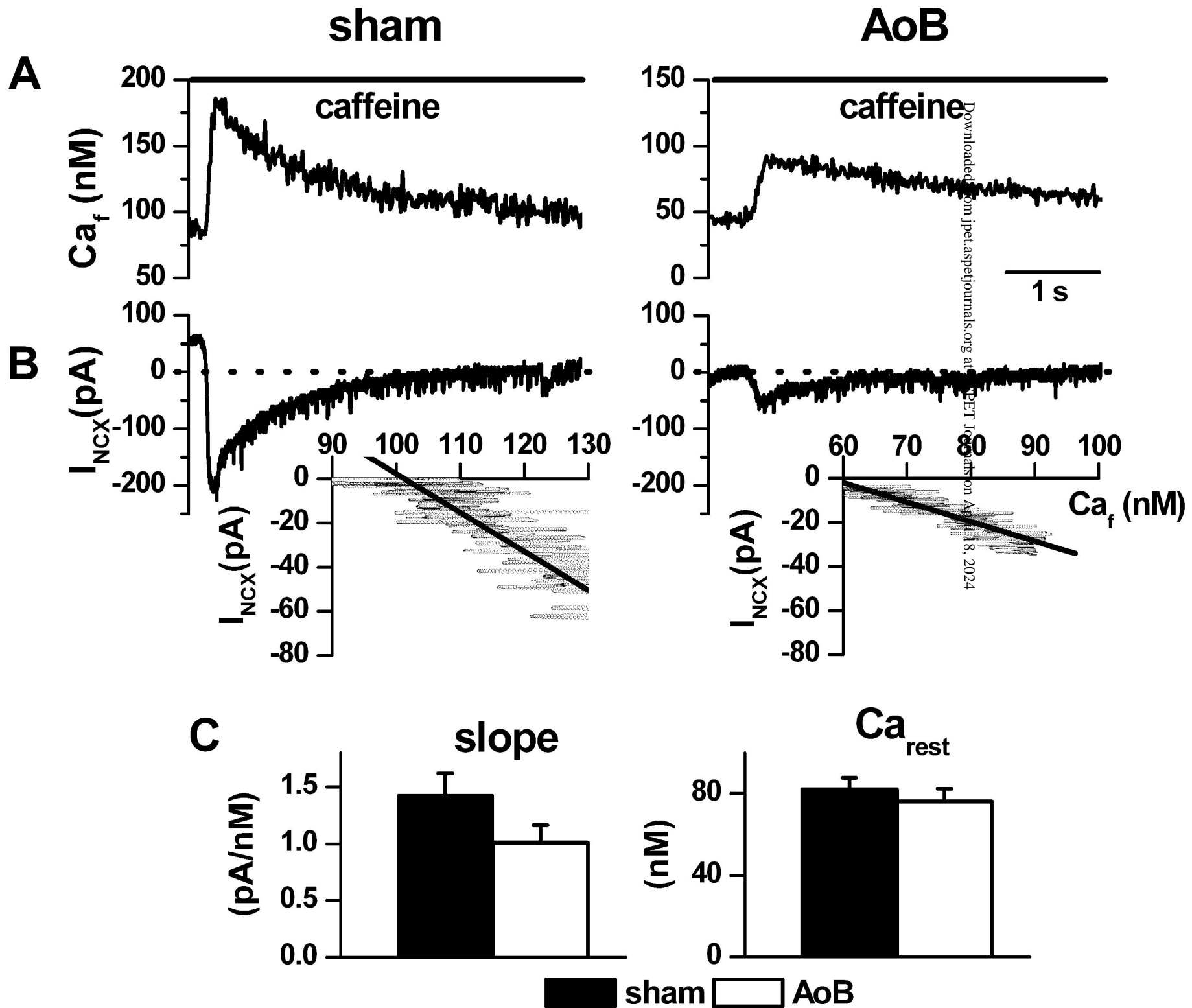


FIG 4

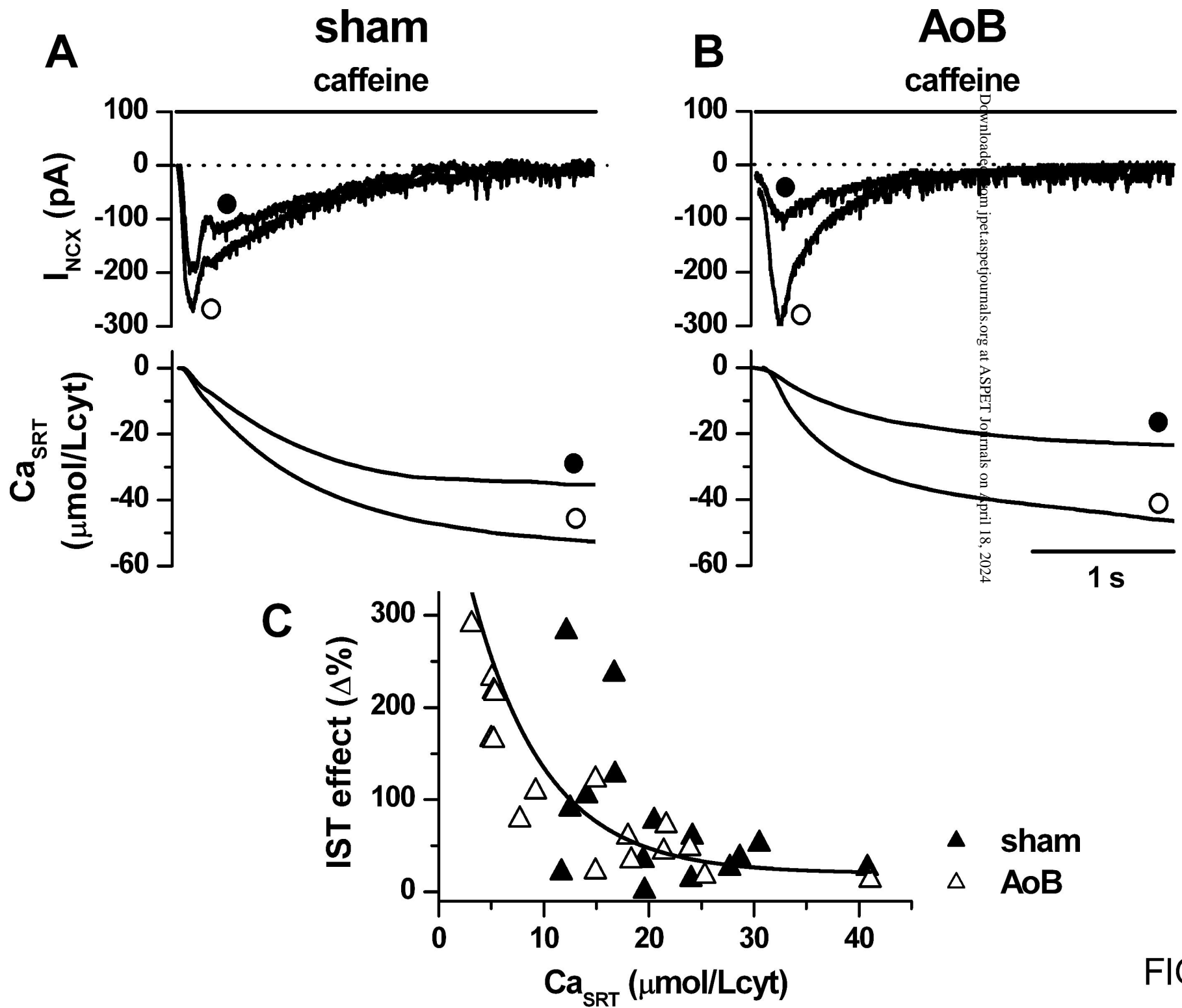


FIG 5

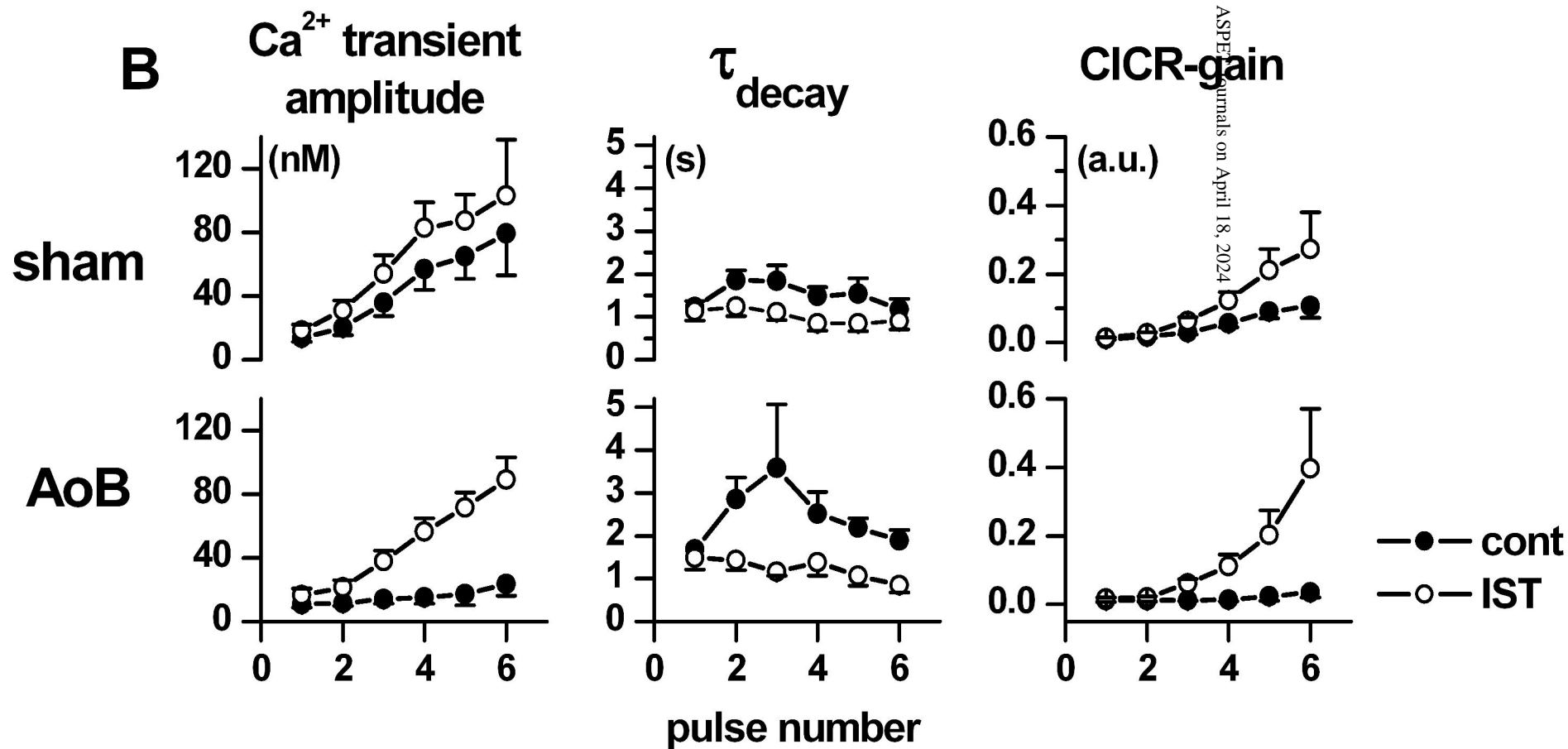
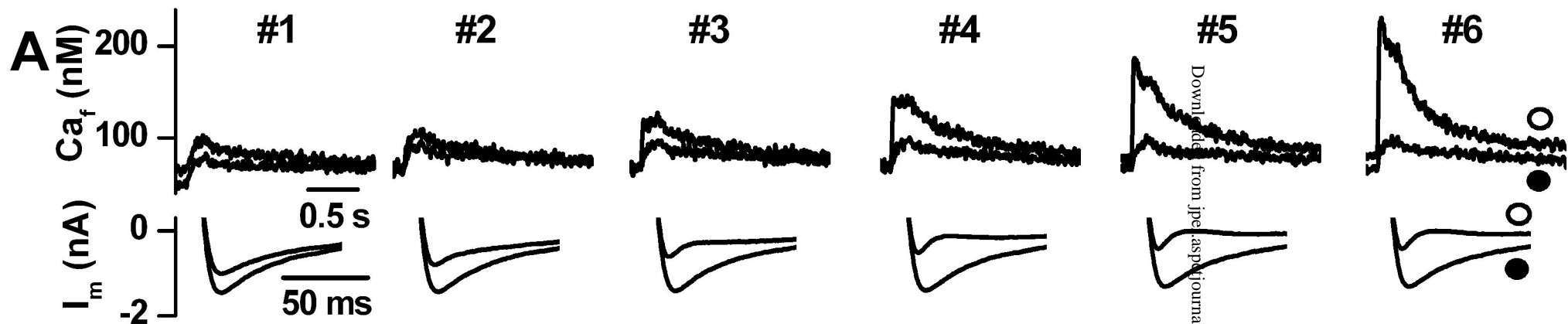


FIG 6

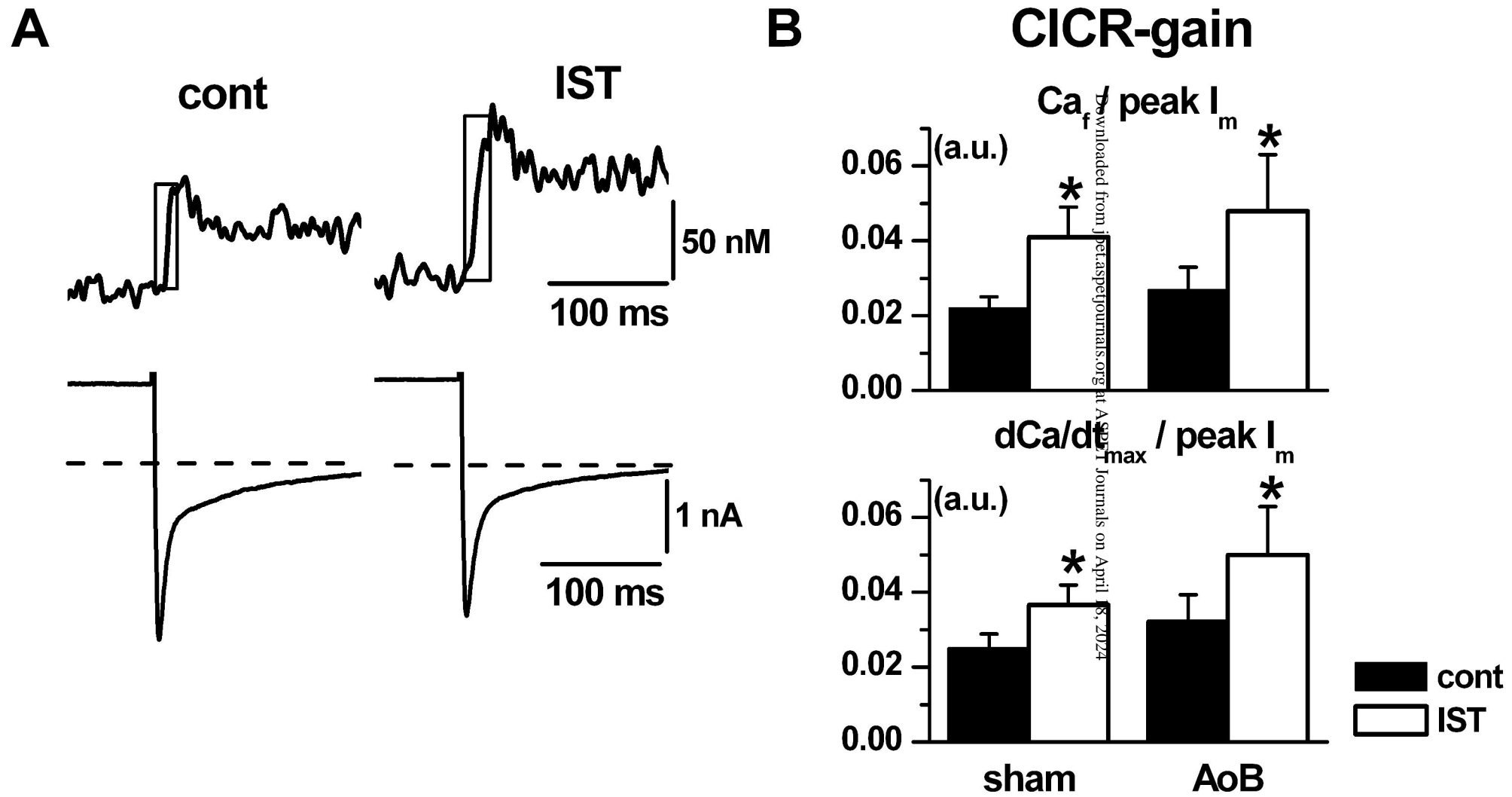


FIG 7

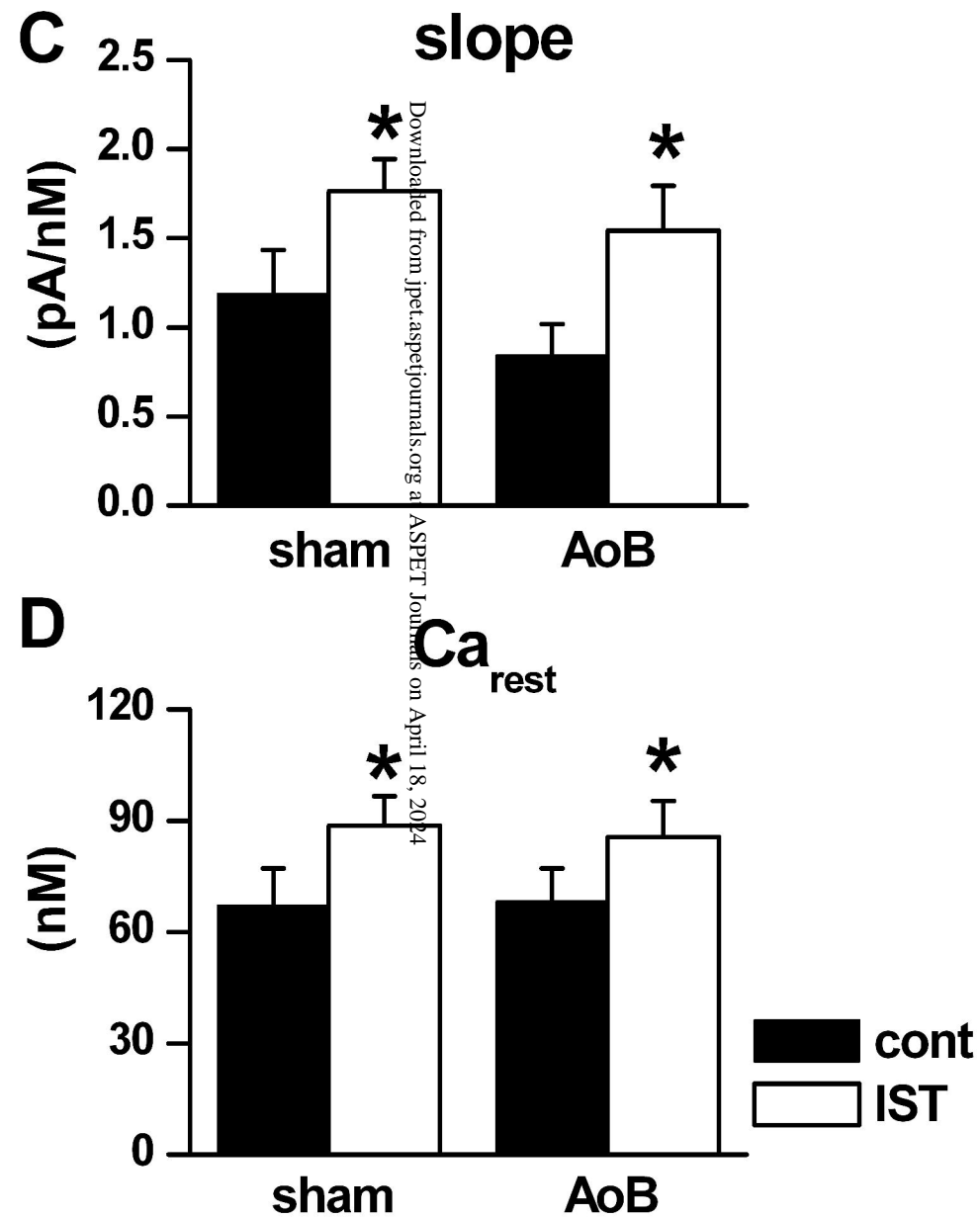
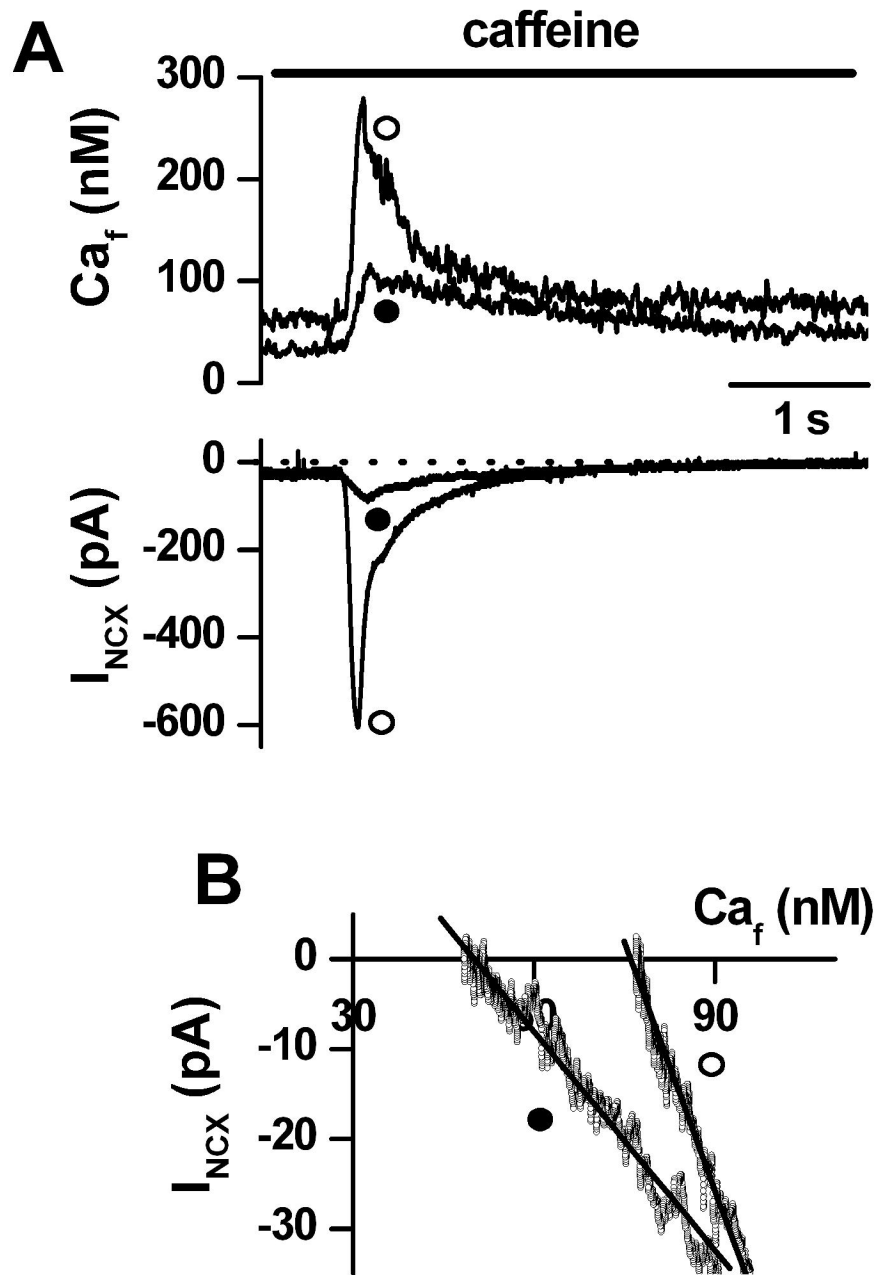


FIG 8